Passivation of GaAs by octadecanethiol self-assembled monolayers deposited from liquid and vapor phases

H. A. Budz
Department of Engineering Physics, McMaster University, Hamilton, Ontario L8S 4L7, Canada

M. C. Biesinger
Surface Science Western, University of Western Ontario, London, Ontario N6A 5B7, Canada

R. R. LaPierre[a)]
Department of Engineering Physics, McMaster University, Hamilton, Ontario L8S 4L7, Canada

(Received 6 January 2009; accepted 23 February 2009; published 20 March 2009)

Self-assembled monolayers (SAMs) of octadecanethiol (ODT), $CH_3(CH_2)_{17}SH$, were deposited on GaAs (100) substrates from liquid and vapor phases. Liquid-phase-deposited SAMs were prepared by immersing the substrate in a dilute solution of ODT and ethanol, while vapor-phase-deposited monolayers were prepared by exposing the GaAs surface to a stream of ODT vapor in an ultrahigh vacuum environment. The structural and optical properties of the resulting SAMs were examined with contact angle (CA) analysis, photoluminescence (PL) spectroscopy, high-resolution x-ray photoelectron spectroscopy (HRXPS), and spectroscopic ellipsometry. Although well-ordered films were formed from both deposition techniques, PL, CA analysis, and ellipsometry measurements revealed that the overall quality, structure, and long-term durability of the resulting SAMs depended on the preparation method. Specifically, time-dependent PL and CA analysis indicated an enhanced stability for vapor-deposited films stored under ambient conditions. Through HRXPS measurements, the attachment of the thiolate molecules to the GaAs substrates was shown to proceed through the formation of chemical bonds at both Ga and As surface sites, with the percentage of each bonding configuration dictated by the surface termination produced via the cleaning process used prior to the SAM deposition. Collectively, the results suggested that more robust monolayers exhibiting greater surface coverage, and therefore increased passivation and stability characteristics, are assembled from vapor phase. © *2009 American Vacuum Society.*
[DOI: 10.1116/1.3100266]

I. INTRODUCTION

The passivation of III-V semiconductor surfaces and, in particular, GaAs has been the subject of intensive studies in recent years.[1–6] The interest in developing durable passivants is mainly derived from the need to remove the high density of problematic oxide-related surface states that originate from the tendency of the semiconductors to oxidize in ambient conditions. Since the defect states detrimentally affect the electronic and optical properties of the materials the role of efficient passivants is critical in enhancing the performance of III-V based devices.[7] Although numerous passivation methods have been proposed, ranging from plasma hydrogenation to inorganic sulfidization, using wet and dry chemical treatments, poor reproducibility, contamination, and rapid degradation under atmospheric conditions have limited the widespread use of these techniques in the processing and fabrication of devices.[1,8,9]

One of the more promising approaches to GaAs passivation involves the deposition of organic self-assembled monolayers (SAMs) on the surface of the semiconductor. The inherent ability of adsorbed monolayers to modify the physical and chemical properties of solid surfaces makes them attractive for the effective control of III-V semiconductors. In particular, alkanethiol-based SAMs have proven to be successful in passivating the electrical activity of unfavorable GaAs dangling bonds through the formation of a well-ordered array of molecules chemically bound to the surface.[10] Consequently, this novel passivation mechanism has demonstrated its relevance as a prospective means of preventing further chemical modification while at the same time maintaining the desired electronic properties of the underlying surface, especially in the case of nanoscale device structures for which there is a large surface-to-volume ratio.[11]

An important consideration in any surface passivation scheme is the stability of the passivating coatings when exposed to ambient conditions. The passivant must inhibit the regrowth of oxide on the semiconductor surface over a prolonged period of time to be a viable candidate for technological applications.[2,12] For SAM-based passivants, a key issue pertains to the precise longevity of the treatments under atmospheric conditions as controversial results have been reported for their effectiveness in protecting III-V surfaces against reoxidation partly due to the range of experimental conditions used to deposit the films across different laboratories.[13–19] Hence, it has become increasingly imperative to accurately determine the stability of SAMs prepared

[a)]Electronic mail: lapierr@mcmaster.ca

by various methods, as well as to develop a better understanding of the reasons underlying the discrepancy in the reliability of the ensuing passivation.

Octadecanethiol (ODT), $CH_3(CH_2)_{17}SH$, SAMs were assembled on GaAs from solution and from vapor phase and the durability and optoelectronic characteristics of the resultant monolayers were evaluated over the course of several months by means of contact angle (CA) analysis and photoluminescence (PL) spectroscopy. Complementary studies using spectroscopic ellipsometry and high-resolution x-ray photoelectron spectroscopy (HRXPS) were conducted to correlate the chemical and structural properties of the films to the efficacy of the resulting passivation.

II. EXPERIMENTAL DETAILS

The crystalline semi-insulating GaAs (100) substrates used in the study were purchased from Wafer Technology Ltd.[20] The ODT (purity: 98+%) was purchased from Sigma-Aldrich[21] and was used without further purification in the solution deposition process.

The self-assembly of ODT monolayers on GaAs samples from liquid phase has previously been described in Ref. 22. Briefly, a clean, UV-ozoned HF-etched substrate was incubated in a 5 mM solution of ODT and anhydrous ethanol with 5% ammonium hydroxide for 48 h at 60 °C. To prevent the regrowth of the native oxide, the thiol solution was purged with nitrogen for several hours to remove the dissolved oxygen before the sample was introduced.

The SAM deposition process as well as the preceding HF etch were carried out in a nitrogen-purged glovebox, with oxygen and moisture levels below 1 ppm, to avoid reoxidation of the freshly etched sample surface, which would otherwise occur in an air ambient. Following the SAM deposition, the sample was rinsed with copious amounts of warm ethanol to remove any physisorbed molecules from the surface and was blown dry with nitrogen.

A custom-made UHV deposition system was used to deposit the SAMs from vapor phase directly onto GaAs substrates. Details regarding the vapor deposition process, as well as the design of the UHV system, are presented in Ref. 22. The growth chamber was equipped with an atomic hydrogen source used for *in situ* surface cleaning of the samples before depositing the SAMs.[23] To probe the nature of the surface modification produced as a result of exposure to atomic hydrogen, a GaAs substrate was treated with atomic hydrogen by the same process used to clean samples prior to depositing SAMs from vapor phase.

With the exception of the stability analysis, all subsequent measurements on the SAM samples were performed either immediately after the preparation of the monolayers or within a couple of days. Between measurements, the samples were stored in an inert nitrogen environment in the aforementioned glovebox.

The experimental data were acquired with a M2000V variable angle spectroscopic ellipsometer manufactured by J. A. Woollam Co., Inc.[24] The ellipsometry measurements were performed over a wide spectral range from 380 to 900 nm. To improve the sensitivity of the measurement to the optical properties and thickness of the film, data were collected at multiple angles of incidence, from 50° to 70°, in increments of 5°. The change in the polarization state of the light upon reflection from the sample surface was measured by means of a rotating compensator, whereas the change in the amplitude was detected by a charge-coupled device (CCD) array. Combining the rotating compensator ellipsometry design with CCD detection allowed for the simultaneous measurement across the entire wavelength range. From the spectra of the ellipsometric angles, Δ and Ψ, the optical properties and the thickness of the monolayers were determined using commercial ellipsometry modeling software supplied by the manufacturer. To increase the accuracy of the results, the measurements were performed at three different locations on each sample, and the calculated parameters were averaged. The details of the parametric model used to estimate the thickness of films are described in Sec. III.

CA goniometry was used to evaluate the characteristics of the SAMs after preparation as well as following an extended exposure to air. The measurement and interpretation of CAs is common practice in the analysis of SAMs as the quality of the films can be determined from this relatively simple experimental procedure. An in-house built goniometer was used to measure the contact angle of a sessile water droplet (5 μl of high-purity de-ionized water) in an air ambient immediately after the deposition of the SAMs. The drop was dispensed through a microsyringe terminated with a blunt-ended needle placed on the surface of the samples. Upon retracting the needle, the static contact angle of the droplet was recorded with a digital camera attached to an optical microscope and the obtained images were analyzed manually. Repeated measurements at three different sample locations indicated a CA precision of $\pm 2°$.

PL spectroscopy was used to assess the passivation properties of the SAMs and to monitor their stability as a function of storage time in air. Luminescence spectra were recorded at room temperature using a home-built apparatus. Continuous excitation was provided by a He–Ne laser source operating at 632.8 nm, while wavelength selection was achieved with a Sciencetech monochromator (model 9050).[25] A silicon photodiode was used to detect the sample luminescence. To incorporate phase sensitivity into the measurement, the laser beam was modulated by a mechanical chopper (200 Hz) and monitored with a lock-in amplifier. A lens was used to focus the laser beam at the sample surface to a spot size of less than 0.5 mm. As absorption of the laser beam occurs close to the top of the sample, the intensity of the resulting PL signal is strongly controlled by the properties of the surface, and hence is indicative of the passivation enhancement following treatment. In order to establish reproducibility between measurements, a highly doped untreated *n*-type GaAs sample was used as a reference against which all PL measurements were compared. The use of a reference standard strongly minimizes the influence of experimental details on the obtained PL results. On each sample, PL was collected from three different locations and averaged to account for any

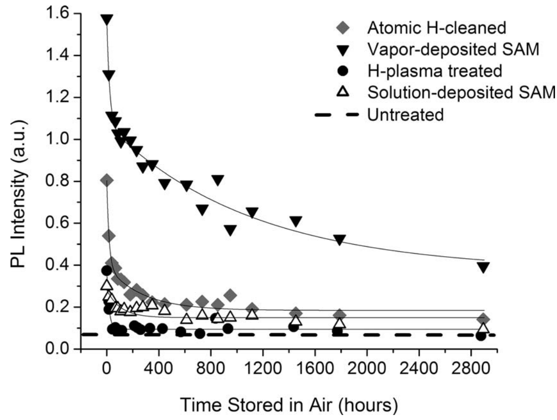

FIG. 1. Room temperature peak PL intensity as a function of storage time in air for ODT SAMs on GaAs prepared from liquid and vapor phases as well as that of untreated and hydrogenated GaAs substrates. The PL data were fitted to exponential decay functions with the fitting results given in Table I.

nonuniformity in the surface properties. The typical variation in peak PL intensity across the surface of each sample was less than 10%.

The bonding chemistry at the SAM-GaAs interfacial regions was analyzed by means of XPS using a Kratos Axis Ultra x-ray photoelectron spectrometer equipped with a monochromatic Al $K\alpha$ (1486.71 eV) source and a charge neutralization system. Survey and high-resolution scans were carried out across a 300×700 μm^2 sample area, with pass energies of 160 and 20 eV, respectively. The data were collected at photoelectron take-off angles of 30° and 90° measured from the sample surface. All spectra were referenced to the GaAs bulk As $3d_{5/2}$ peak at 40.95 eV.

III. RESULTS AND DISCUSSION

To determine the stability of the passivating films, the PL intensity was measured after leaving the samples under ambient conditions. Figure 1 shows the peak PL intensity as a function of storage time in air for ODT SAMs on semi-insulating GaAs prepared from liquid and vapor phases, as well as that of untreated and atomic-hydrogen-cleaned GaAs substrates. As indicated in the figure, the PL intensity progressively decreased over the measurement time for all of the treated samples. The time dependence of the PL intensity decay for the vapor-deposited SAM and the atomic-hydrogen-cleaned sample exhibits temporal characteristics with two different rate components. Specifically, the decrease in the luminescence signal appears to proceed at a faster rate initially within the first ~100 hours and then continues at a slower rate with increased exposure to an ambient environment. To highlight this relationship, the PL data were fitted using a least-squares fitting routine to a double exponential decay equation as defined by[26]

$$\text{PL intensity} = \alpha_o + A_1 e^{-t/\tau_1} + A_2 e^{-t/\tau_2}, \qquad (1)$$

where t is the storage time in air, A_1 and A_2 are positive fit parameters, and τ_1 and τ_2 are the fast and slow decay time constants, respectively. As demonstrated by the results of the fit analysis presented in Table I, the time constant τ_1 calculated for the luminescence decay of the vapor-deposited SAM closely resembles that of the atomic-hydrogen-cleaned sample. As described below, the fast decay (τ_1) can be attributed to the hydrogen passivation, while the slower decay (τ_2) can be explained by ODT passivation.

In an effort to clarify the role of the hydrogen in the observed PL enhancement and to eliminate the influence of residual ODT in the vapor deposition chamber, a GaAs substrate was exposed to a hydrogen plasma source in a clean, ODT-free UHV reactor. The processing conditions of the hydrogen plasma treatment were set equivalent to those used for the atomic hydrogen cleaning in order to achieve an analogous resultant surface. Specifically, the plasma treatment was performed for 10 min at a rf (13.56 MHz) power of 350 W applied in the inductively coupled mode at a pressure of 2.4×10^{-5} Torr and a substrate temperature of approximately 500 °C. As the data in Fig. 1 show, the peak PL intensity measured immediately following the plasma treatment increased compared to the untreated substrate. The improvement in PL signal exhibited by the hydrogenated sample is attributed to the passivation of the dangling bonds and/or near-surface lattice defects in the GaAs substrate by hydrogen atoms. However, with a longer exposure to an ambient atmosphere, the PL yield of the plasma-treated sample rapidly decayed (within about 48 h) and reverted to nearly the same level as that of an untreated substrate.

To quantify the dynamic characteristics of the PL signal, the time-dependent PL data measured on the hydrogen plasma passivated sample were best fitted to a single exponential equation as given by

$$\text{PL intensity} = \alpha_o + A_1 e^{-t/\tau_1}, \qquad (2)$$

where t is the storage time in air, A_1 is a positive fit parameter, and τ_1 is the decay time constant. The results of this

TABLE I. Parameters obtained from the fit analysis of the PL decay measurements for the SAM-modified and hydrogenated GaAs samples.

Sample	Curve-fitting equation	Parameters calculated from curve-fitting analysis				
		α_o	A_1	τ_1 (h)	A_2	τ_2 (h)
Vapor-deposited SAM	$\alpha_o + A_1 e^{-t/\tau_1} + A_2 e^{-t/\tau_2}$	0.37 ± 0.08	0.51 ± 0.06	22 ± 6	0.70 ± 0.07	$(1.1\pm0.3)\times10^3$
Atomic hydrogen cleaned	$\alpha_o + A_1 e^{-t/\tau_1} + A_2 e^{-t/\tau_2}$	0.18 ± 0.01	0.41 ± 0.04	17 ± 4	0.21 ± 0.03	$(2.7\pm0.9)\times10^2$
Hydrogen plasma treated	$\alpha_o + A_1 e^{-t/\tau_1}$	0.10 ± 0.01	0.28 ± 0.02	17 ± 2	⋯	⋯
Solution-deposited SAM	$\alpha_o + A_2 e^{-t/\tau_2}$	0.15 ± 0.01	⋯	⋯	0.13 ± 0.02	$(1.1\pm0.3)\times10^2$

analysis are summarized in Table I and indicate that the partial degree of passivation provided by the hydrogen treatment alone is not successful in stabilizing the GaAs surface for an extended period of time. It is important to note that the time scale (τ_1) over which the PL intensity of the plasma-processed sample degrades coincides within the limits of experimental error to the fast decay rates observed on the atomic-hydrogen-cleaned sample and the vapor-deposited SAM. The fact that all three of these samples were submitted to a hydrogen treatment suggests that the mechanism responsible for the initial decline of the PL signal is the same in all three cases and most likely involves a rapid reduction of the passivation efficacy provided by the hydrogen atoms with increased exposure to air.

Upon closer examination, the experimental data shown in Fig. 1 reveal that the SAM-modified samples are more stable when compared to the hydrogen-plasma-treated sample. In particular, the time required for the PL intensity to decay to 60% of its initial value was 109 h for the solution-deposited SAM and only about 16 h for the plasma-treated sample, even though the PL signal initially increased by a larger factor following hydrogen plasma passivation. Clearly, it can be concluded that the relative improvement in the luminescence efficiency brought about solely by the introduction of hydrogen is short lived while the enhancement in PL intensity due to the solution-deposited thiol monolayer in the absence of any hydrogen treatment is maintained for a longer duration. The apparent long-term stability of the SAM-passivated surfaces is believed to result from the formation of robust bonds between the sulfur containing thiols and the GaAs surface, which act as an effective barrier against oxidation of the underlying surface. In the case of the atomic-hydrogen-cleaned sample, the PL decay data revealed an initial fast decay (τ_1) due to hydrogen passivation and a slower decay (τ_2). The slower decay can be explained by the deposition of a partial ODT film resulting from residual thiols present in the deposition chamber. The existence of thiol species in the preparation chamber during the atomic hydrogen cleaning process was confirmed by mass spectrometry and is thought to result from the liberation of ODT molecules condensed on the inner surfaces of the chamber from previous SAM depositions.[22]

Another important outcome that can be inferred from the luminescence dynamics deals with the relative stability of the vapor-deposited SAM compared to its solution-deposited counterpart. As shown in Fig. 1, the magnitude of the PL improvement induced by the SAM was a factor of 5 greater for vapor deposition when compared to that from solution deposition. After a few hours in an ambient environment, the decay in the luminescence intensity was more pronounced for the vapor-deposited SAM than the solution-deposited SAM. However, with extended ambient exposure time this decay rate decreased significantly. In contrast, the PL signal measured on the monolayer deposited from solution decreased at a more gradual rate initially and then reached a steady-state level after roughly 65 h in air. This difference in the stability characteristics between the samples can be explained by the variation in the processing conditions used during the deposition of the films. In the case of the vapor-deposited monolayer, the sample was pretreated in atomic hydrogen prior to the deposition of the thiol film. Consequently, the ensuing passivation of the GaAs surface immediately following the vapor deposition is a product of two distinct passivation methods, namely, hydrogen passivation and ODT SAM passivation. As shown previously in the case of the hydrogen-plasma-treated sample, the effects of hydrogen passivation dissipate quickly, and thus are likely responsible for the initial abrupt decrease in the PL intensity of the vapor-deposited sample. With an extended exposure to ambient conditions, the decay in PL yield drastically reduced to a value lower than the rate exhibited by the solution-deposited SAM (see Table I), which suggests that the prolonged enhancement in PL can be attributed to the passivation of the underlying substrate by the organic monolayer. Moreover, after 4 months in air, the final PL intensity observed on the vapor-deposited SAM was still about a factor of 5 greater than the intensity measured on the solution-deposited SAM. On the basis of this comparison, the PL results indicate that more stable films with better surface coverage are produced from vapor than from liquid phase and that the hydrogen cleaning process alone is not responsible for the improved PL intensity.

TABLE II. Static water CAs measured on GaAs following various treatments and SAM deposition methods. The CAs were measured on newly treated surfaces as well as after being exposed to air for a 4 month period.

Sample	CA (±2°) (deg)	
	Initial[a]	After 4 months in air[b]
Untreated	73	···
Hydrogen plasma cleaned	62	75
Atomic hydrogen cleaned	95	82
Solution-deposited SAM	100	85
Vapor-deposited SAM	104	98

[a]Measured on newly treated surfaces.
[b]Measured after being exposed to air for a 4 month period.

To validate the conclusions regarding the stability of the organic films, CA analysis was used to detect the changes in wetting properties on the functionalized semiconductor surfaces brought on by the exposure of the samples to ambient conditions. The static water CAs measured on the various GaAs surfaces are summarized in Table II. Immediately after the SAM deposition, the ODT monolayers prepared from liquid and vapor phases demonstrated static water CAs of 100° and 104°, respectively. According to a survey of literature, water CAs in excess of 100° indicate the formation of high-quality ODT SAMs on GaAs surfaces.[15,27,28] Consequently, the measured CAs suggest a similar initial structure for monolayers prepared from liquid and vapor phases, consistent with the existence of uniform films chemically bonded to the GaAs surface. Nevertheless, the small difference between the water CAs on the two SAMs could be interpreted to reflect a statistically significant difference in

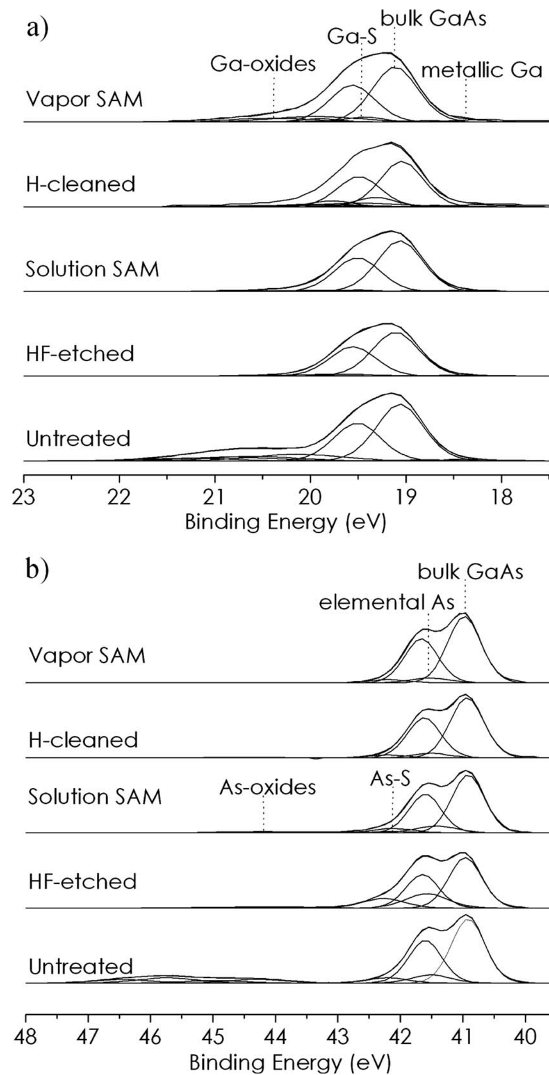

FIG. 2. HRXPS spectra of the (a) Ga 3*d* and (b) As 3*d* core levels of GaAs after various treatments and SAM preparation methods recorded at a take-off angle of 90°. The spectra have been offset vertically for clarity and fitted to show the contributions of the component features.

the packing density of the monolayers, as discussed in Ref. 22. While the CA measured on the atomic-hydrogen-cleaned sample was smaller than that observed on the ODT SAMs, it is larger than the CA measured on the untreated substrate, as well as that measured on the hydrogen-plasma-treated GaAs surface. Thus, the increased hydrophobicity of the sample surface provides support for the hypothesis that the enhancement in PL intensity obtained on the atomic-hydrogen-cleaned GaAs sample is due in part to the formation of a partial ODT monolayer.

As shown in Table II, the CA of the SAM-modified surfaces decreased after the samples were stored in air for a period of 4 months. Since the magnitude of the CA depends directly on the quality of the SAM monolayer, the decrease in the CA represents degradation in the film structure with prolonged exposure to the air ambient. Accordingly, the smaller change in the CA observed for the vapor-deposited monolayer compared to that synthesized from solution reflects the superior stability of SAMs prepared under UHV conditions and is consistent with the PL findings discussed earlier which show a more gradual disruption of the film deposited from vapor phase over the course of several months.

TABLE III. Binding energies of different peaks in the Ga 3*d* and As 3*d* spectra presented in Figs. 2 and 3. For simplicity, only the energy of the main component in each doublet is reported.

Core level	Binding energy (eV)	Peak assignment
Ga $3d_{5/2}$	19.1 ± 0.2	Bulk GaAs
	20.8 ± 0.1	$Ga(OH)_3$
	20.0 ± 0.3	Ga_2O_3
	19.8 ± 0.1	Ga_2O
	18.4 ± 0.2	Metallic Ga
	19.5 ± 0.2	Ga–S
As $3d_{5/2}$	40.9 ± 0.1	Bulk GaAs
	46.2 ± 0.3	As_2O_5
	44.4 ± 0.4	As_2O_3
	41.5 ± 0.3	Elemental As
	42.1 ± 0.1	As–S

To more fully understand the consequences of GaAs passivation by ODT SAMs, the chemical composition of the monolayers deposited from vapor and liquid phases was examined by HRXPS. Figures 2(a) and 2(b) show a comparison of Ga 3*d* and As 3*d* core-level spectra, respectively, for GaAs samples which have been untreated, freshly etched in buffered HF, exposed to atomic hydrogen, and modified with an ODT monolayer. The spectrum of the HF-etched GaAs surface was obtained from a sample that was etched for 2.5 min in concentrated (~49%) HF, rinsed in de-ionized water, dried in air, and loaded into the vacuum atmosphere of the XPS instrument within approximately 3–5 min. Since the etched sample was exposed to the ambient environment for a minimal duration, it was used as a reference standard to which the amount of oxide present at the surface of the other samples was compared. The measured Ga 3*d* and As 3*d* spectra were decomposed into several distinct components, with each fitted self-consistently by a pair of characteristic doublets. Peak assignments were made to account for contributions from the bulk Ga and As species, native oxide Ga and As species, elemental Ga and As species, as well as from specific Ga–S and As–S binding components, where applicable. The binding energies associated with the core emissions are summarized in Table III. A survey of recent literature shows that the peak assignments are in agreement with previously reported values.[4,29–31] The fitted spectra overlapped nearly perfectly with the measured spectra in Fig. 2. Due to the good quality of the fit to the experimental data, some important trends are deduced from the following analysis.

To accentuate the differences between the various surface treatments, the signals from the Ga/As oxides, metallic Ga/elemental As, and Ga–S/As–S components are displayed separately in Fig. 3. The spectra in Fig. 3 were multiplied by

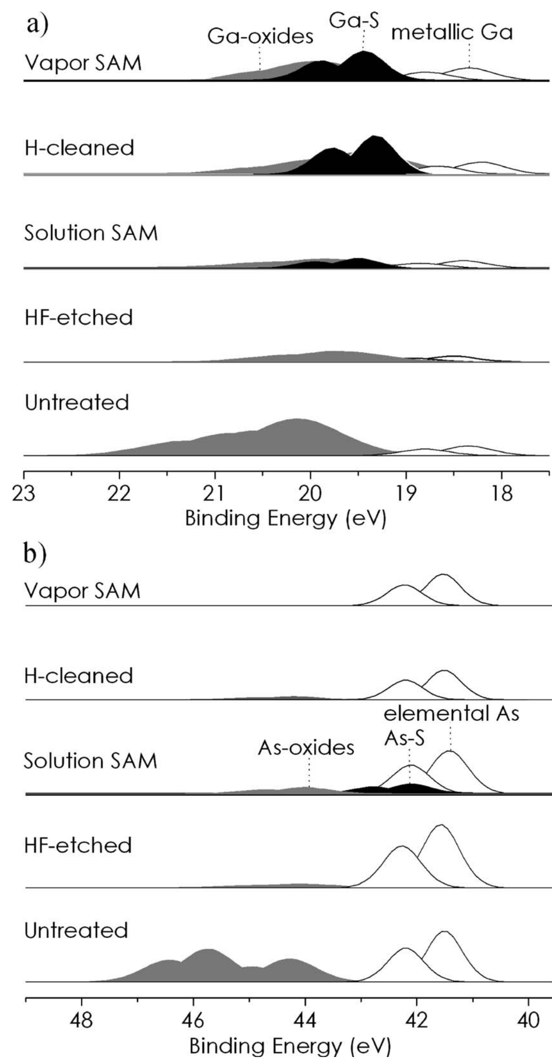

FIG. 3. HRXPS spectra of specific (a) Ga 3*d* and (b) As 3*d* core levels of GaAs after various treatments and SAM preparation methods recorded at a take-off angle of 90° (gray doublet: Ga/As oxides, white doublet: metallic Ga/elemental As, black doublet: Ga–S/As–S). The spectra have been offset vertically for clarity. The signals from the Ga/As oxides, metallic Ga/ elemental As, and Ga–S/As–S components have been multiplied by a factor of 5 relative to those shown in Fig. 2 to accentuate the differences between the curves.

a factor of 5 relative to those in Fig. 2. As shown in Fig. 3, the untreated GaAs substrate is heavily oxidized at the surface by a native oxide layer consisting of a mixture of Ga- and As-related species. After the etching in HF, the quantity of oxide on the surface was greatly reduced, although it was not entirely eliminated. The incomplete removal of the native oxide layer is likely due to the short exposure of the sample to air during its transfer into the XPS system. Following the deposition of the ODT monolayer from solution, the amount of oxide stayed virtually the same as that measured on the etched material. The fact that the level of oxidation remained unchanged suggests insufficient etching of the residual oxide by the ammonium hydroxide in the thiol solution. As the presence of oxide species on the sample surface is believed to hinder the formation of the monolayer,[32] it is likely that the packing density of the solution-deposited film is less than that of an ideal monolayer formed on an oxide-free surface. On the other hand, the spectra for the vapor-deposited SAM presented in Fig. 3 show a greater contribution from the Ga oxide component in comparison to that of the HF-etched sample, as well as the total elimination of the As oxide component. Since similar results were obtained for the atomic-hydrogen-cleaned sample, it is believed that the selective removal of the As oxide species is associated with the exposure of the GaAs surface to atomic hydrogen. Hydrogenation of a GaAs substrate causes a reaction between the incident hydrogen atoms and the native oxide, which leads to a reduction in the concentration of more volatile As species and results in regions of Ga oxide, specifically Ga_2O_3, on the surface.[33,34] The fact that the Ga oxides tend to remain partially intact following hydrogenation is considered to play a role in preserving the effects of hydrogen passivation.[9,35] Consequently, as the XPS data indicate, the atomic hydrogen pretreatment was not effective in fully reducing the oxides of Ga presumably due to the processing conditions used during the treatment, such as substrate temperature and/or insufficient hydrogen dose, which may not have been adequate to completely desorb the Ga_2O_3.[36] The existence of a non-negligible amount of Ga oxide on the hydrogenated samples suggests that the atomic hydrogen cleaning process can be further optimized to promote the full removal of Ga-like oxides, potentially increasing the coverage of SAMs subsequently deposited on the pretreated surfaces. Alternatively, the Ga oxide in the spectra of the hydrogen-treated samples can be explained by the short exposure of the samples to the ambient during their transfer into the XPS system. When the GaAs surface is exposed to atomic hydrogen at an elevated temperature, the selective depletion of As-related species occurs, which leads to the production of a Ga-rich overlayer on the resultant surface, as discussed below. Consequently, the Ga oxide could have in fact been reduced as a result of the hydrogen treatment and simply reformed rapidly on the ODT-free Ga enriched areas during the short exposure of the samples to air. A method of controlling and monitoring the atomic hydrogen cleaning process involves the introduction of an *in situ* characterization technique, such as reflection high-energy electron diffraction or Auger electron spectroscopy, during the treatment in order to define the optimal conditions for the cleaning process, as well as to determine the end point of the oxide removal.[37]

Another interesting feature in Fig. 3 is the appearance of a peak at 18.4 eV in the HRXPS spectra of the hydrogenated samples that can be assigned to elemental Ga generated by the selective depletion of As from the substrates during the hydrogen treatment.[35,36] Along with the existence of a metallic component, the Ga spectra of the hydrogen-cleaned sample and that of the vapor-deposited SAM reveal a small peak at an energy of 19.5 eV. As this peak was not observed in the spectra of the untreated substrate and the HF-etched sample, it was attributed to the formation of Ga–S bonds on the GaAs surface. This value for the binding energy of Ga–S is in accordance with that previously observed for sulfides on GaAs.[4] The presence of Ga–S bonds in the spectrum of the

hydrogen-cleaned sample confirms the formation of a partial ODT film on the sample surface, as speculated above. In contrast to the Ga spectra, the As spectra of the hydrogen pretreated samples do not indicate the existence of an As–S binding component. The dominant contribution from the Ga–S bonding and the absence of As–S bonding from the spectrum of the vapor-deposited SAM is expected when the stoichiometry of the surface prior to the film growth is considered. As mentioned previously, the hydrogen-cleaned GaAs surface is depleted of As as a result of the cleaning process, and thus is Ga enriched. Since the deposition of the SAM from vapor phase immediately follows the hydrogen treatment, it is not surprising that the majority of the chemical bonds at the SAM-GaAs interface are Ga–S in nature due to the lack of available As bonding sites on the cleaned surface. Conversely, the Ga 3*d* and As 3*d* spectra of the solution-deposited SAM shown in Fig. 3 indicate a relatively equal quantity of Ga–S and As–S bonds following ODT modification. This result is also anticipated as previous reports indicate that the chemical etching of GaAs in a dilute HF solution produces a nearly stoichiometric surface termination with a slight excess of As atoms.[38] It should be noted that the HF-etched sample used in the XPS analysis was produced by etching a GaAs substrate in a solution five times more concentrated than that used to clean the sample prior to depositing the SAM from liquid phase. Since the As enrichment on the resultant surface is proportional to the concentration of HF,[39] the etched surface in Fig. 3 is expected to be significantly more As rich than that used in the solution deposition of the ODT film, which should reflect a more stoichiometric surface composition. Therefore, the XPS data seem to suggest that S-based chemical bonds between the thiolate molecules and the GaAs surface occur at both Ga and As adsorption sites, with the relative abundance of each bonding configuration strongly dependent on the surface composition achieved by the cleaning method used prior to the deposition of the SAM.[40] Moreover, since Ga–S bonds have been reported to be stronger than As–S ones, the fact that Ga–S bonds are more prevalent in the monolayer deposited from vapor phase is consistent with the increased durability of the SAM, as evident in the PL and CA measurements.[4,41,42]

A comparison of the C 1*s* and O 1*s* spectra of the analyzed samples is given in Fig. 4. After etching in the HF solution, the C 1*s* spectrum of the GaAs substrate shows the presence of carbon contamination as defined by existence of the main hydrocarbon-related peak at a binding energy of 285.0 eV, as well as the formation of a higher energy tail which can be attributed to oxidized carbon species in the form of CO and CO_2 at about 286.5 and 289.1 eV, respectively.[43] Contamination of the freshly etched surface by adventitious carbon probably occurred during the transfer of the sample into the XPS apparatus. On the other hand, the C 1*s* spectra of the atomic-hydrogen-cleaned sample as well as those of the SAM-modified samples show a complete absence of oxidized carbon and the distinct presence of a single sharp peak at a binding energy of approximately 284.7 eV,

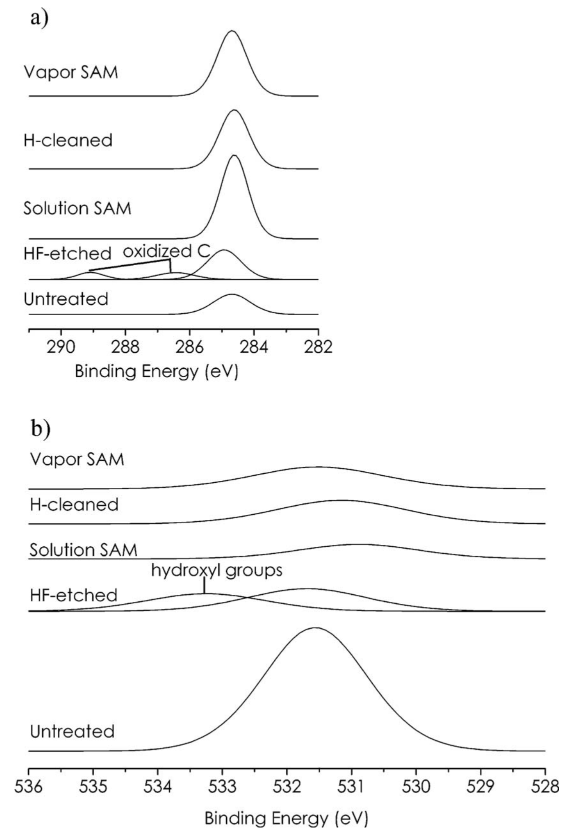

FIG. 4. HRXPS spectra of the (a) C 1*s* and (b) O 1*s* core levels of GaAs after various treatments and SAM preparation methods recorded at a take-off angle of 90°. The spectra have been offset vertically for clarity.

which agrees well with the binding energy reported for C–C/C–H bonds in the backbone of ODT SAMs on GaAs.[18,19]

The lower intensity of the C 1*s* emission for the hydrogen-cleaned sample when compared to that for the ODT-treated samples signifies the existence of a partial ODT film with a lower surface coverage. In addition, the C 1*s* peaks of the hydrogen-cleaned and solution-deposited SAM samples are slightly shifted to a lower binding energy with respect to that of the vapor-deposited SAM, which suggests that the carbon atoms exist in an alternate chemical state and likely reflects a more disordered structure for the thiolate molecules on the surfaces of these samples. Moreover, the larger intensity of the C 1*s* peak observed on the solution-deposited SAM when compared to that of the vapor-deposited SAM may be interpreted in terms of a difference in the tilt angle of the alkyl chains comprising both monolayers. The larger intensity of the C 1*s* line on the SAM prepared from solution can reflect a thicker monolayer structure, and thus a smaller tilt of the alkyl chains from the surface normal. In contrast, the smaller intensity of the C 1*s* signal on the vapor-deposited SAM suggests a more canted, thinner film structure with a larger angle between the chain axis and the surface normal. The presumed difference in the orientation of the monolayers relative to the sample surface was verified by spectroscopic ellipsometry as discussed later.

The O 1*s* spectra shown in Fig. 4 provide further support for the conclusions deduced from the respective Ga 3*d*,

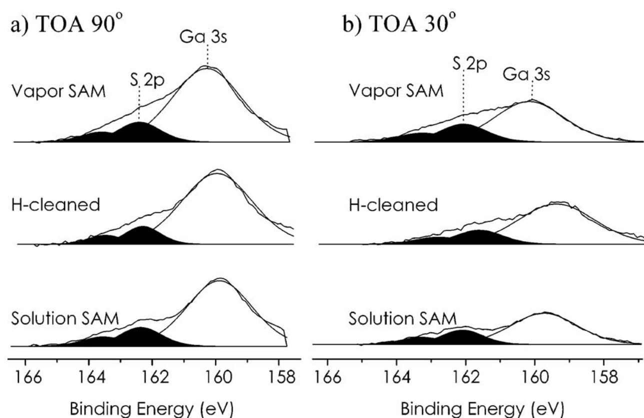

FIG. 5. HRXPS spectra of the S 2*p* region for the SAM-modified and hydrogen-cleaned GaAs samples recorded at take-off angles of (a) 90° and (b) 30°. The spectra have been offset vertically for clarity (TOA: take-off angle) (white peak: Ga 3*s*, black doublet: S 2*p*).

TABLE IV. Ratios of elements calculated from the integral intensities of the main peaks in the respective angle-dependent XPS spectra.

Sample	Ratio of elements	Take-off angle 90°	Take-off angle 30°
	C/S	6.5	9.0
Atomic hydrogen cleaned	C/O	1.4	3.0
	C/S	6.8	12.1
Solution-deposited SAM	C/O	3.2	5.2
	C/S	5.4	8.3
Vapor-deposited SAM	C/O	1.6	3.3

As 3*d*, and C 1*s* spectra. In particular, the O 1*s* data clearly show that the amount of surface oxide is significantly diminished following SAM modification and atomic hydrogen cleaning when compared to the level obtained after etching in HF, as well as to the initial level on the untreated GaAs substrate. As these data are consistent with minimal levels of Ga- and As-related oxides in the Ga 3*d* and As 3*d* spectra of the SAM-passivated samples, it provides evidence for the previous statement concerning the ability of the films to act as effective barriers against oxidation of the underlying surface. It is interesting to note in Fig. 4 that in addition to the main oxygen component, the spectrum of the HF-treated sample shows the existence of hydroxyl groups on the etched GaAs surface, as indicated by the presence of the higher binding energy component at about 533.3 eV.[44]

The larger intensity of the O 1*s* core peak for the hydrogen-cleaned sample when compared to that from the SAM-modified samples coincides with the formation of an islandlike ODT coating. Likewise, the slightly larger intensity of the O 1*s* signal for the vapor-deposited SAM than for the solution-deposited monolayer correlates well with the aforementioned assumption regarding the difference in the tilt angle of the monolayers.

In addition to investigating chemical bonding of the SAMs in the Ga 3*d* and As 3*d* energy regions, the adsorption of the thiols to the GaAs substrates was evaluated by examining the S 2*p* energy region. Figure 5 shows the XPS spectra of the SAM-modified surfaces as well as that of the hydrogen-cleaned sample in the vicinity of the S 2*p* core level. To enhance surface sensitivity of the measurement, an additional set of spectra was acquired at a take-off angle of 30°, measured between the sample surface plane and the entrance to the detector. To distinguish the relative contributions of the main components, the spectra were deconvolved into two main constituents representing signals from the Ga 3*s* and S 2*p* levels. Due to limitations in the energy range surveyed, contributions from the As plasmons was not included in the fitting routine. Since the shift in energy between the Ga 3*s* and S 2*p* levels is small (~3 eV) there exists a degree of overlap between the peaks which makes the analysis less straightforward. Nevertheless, the appearance of a small doublet at a binding energy of approximately 162 eV is clearly evident in Fig. 5, consistent with previously reported values for the S $2p_{3/2}$ and S $2p_{5/2}$ components on GaAs.[31,45] Insufficient resolution and signal-to-noise characteristics of the XPS system prevented unambiguous decomposition of the core peaks into specific Ga–S and As–S chemical states. The aforementioned instrumental limitations notwithstanding, the existence of the S 2*p* features in the spectra of the ODT-treated samples confirms the formation of direct thiolate bonds with the GaAs surface, as exhibited in the respective Ga 3*d* and As 3*d* spectra. Furthermore, the observation of the S 2*p* peaks in the spectrum of the hydrogen-cleaned sample further substantiates the conclusion that the residual thiols present in the UHV chamber chemically bond to the freshly cleaned substrate.

The nature of the thiolate-GaAs bonds was assessed to a greater extent by reducing the take-off angle of the XPS measurement to 30°. By decreasing the take-off angle of the photoelectrons, the surface sensitivity of the XPS measurement can be increased. As the line shapes and position of the peaks remained similar to that obtained at the 90° take-off angle, for the sake of brevity, only the spectra in the S 2*p* region are shown in Fig. 5 for the hydrogen-cleaned and SAM-passivated samples. As expected, the intensity of the S 2*p* and Ga 3*s* peaks decreased concomitantly with the relative decrease in the sampling depth. However, the contribution of S-related features to the overall spectra increased relative to the bulk Ga component, demonstrating that the sulfur headgroups lie closer to the surface immediately above the GaAs interface.

From the integrated intensities of the S 2*p*, C 1*s*, and O 1*s* peaks, the C/S and C/O ratios were derived for each sample and summarized in Table IV. The area intensity ratios were calculated using the appropriate sensitivity factors, assuming that the C 1*s* and O 1*s* signals originated entirely from the organic film and oxide regions, respectively. Due to the ambiguity in the curve fitting of the sulfur species along with lateral inhomogeneities of the SAM films, the derived ratios indicate qualitative trends in the depth profile of the surface region and do not provide quantitative information regarding film properties, such as the thickness. Nonetheless, an estimate of the elemental distribution perpendicular to the

sample surface can be obtained and provides the basis for a useful model of the molecular architecture. As shown in Table IV, the ratio of C/S increased with a reduction of the take-off angle. The attenuation of the S 2*p* signal can be attributed to the inelastic scattering of the photoelectrons by alkyl chains oriented away from the GaAs-bound sulfur headgroup toward the surface. As compared to the solution-deposited SAM, the smaller change in the C/S ratio observed on the vapor-deposited SAM and the hydrogen-cleaned substrate implies a larger inclination of the thiolate molecules on the surfaces of these samples. Similarly, at the lower take-off angle, the C/O ratio for each of the samples increased, indicating that, on average, the oxygen atoms lie closer to the GaAs interface than the carbon atoms. These results correlate with the corresponding Ga 3*d* and As 3*d* spectra and suggest that despite the pretreatments (e.g., HF etching or exposure to atomic hydrogen) used to remove the native oxide prior to the deposition of the monolayers, regions of oxide remained on the GaAs surface, which may have perturbed the subsequent anchoring of the thiols. The fact that the presence of residual oxides was observed on films formed from both liquid and vapor phases indicates that the preparation methods used before either deposition technique require further optimization, which may improve the overall quality of the resultant SAMs.

The properties of the monolayers deposited from liquid and vapor phases were further investigated by ellipsometry measurements. To describe the optical properties of the vapor-deposited SAM, a four-phase (ambient/SAM/interface/substrate) model was used based on the surface chemistry deduced from the XPS analysis presented above. A porous GaAs interface layer was included in the analysis to represent the hydrogen-induced changes in the optical properties of the surface as a result of the cleaning process. The interface layer accounts for the interaction of atomic hydrogen with the near-surface regions by means of structural incorporation, surface roughening, defect passivation, and modification of the surface geometry.[36,46,47] For layers composed of more than one constituent, the Bruggeman effective medium approximation (BEMA) was used to model the optical properties of the composite layer. The optical constants for the oxide-free semi-insulating GaAs substrate were obtained by ellipsometry from a freshly HF-etched sample. A Cauchy dispersion function was used to describe the wavelength-dependent index of refraction of the thiols, with the appropriate coefficients obtained from previous work.[22] The fitting parameters in each model were determined by minimizing the mean square error with the provided regression analysis software. Realistic physical constraints were imposed on parameters to further increase the validity of the models. For example, the index of refraction of the ODT was maintained at a real value, as alkanethiols are nonabsorbing in the wavelength range of interest.[48]

Figure 6 shows the experimental and the model-generated Δ and Ψ spectra for the vapor-deposited SAM sample. A schematic of the corresponding model used to fit the measured spectra is also presented in the figure, along with the

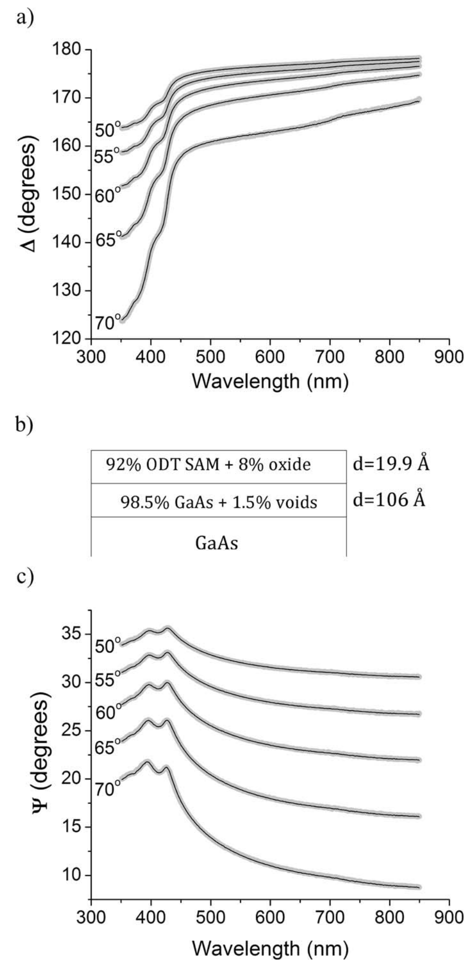

FIG. 6. Spectra of ellipsometric parameters (a) Δ and (c) Ψ of a vapor-deposited ODT SAM on GaAs for various angles of incidence (thick gray line: experimental data, thin black line: model fit). In (b) the best-fit BEMA model to the corresponding spectra is shown.

respective best-fit layer thicknesses and compositions. As is evident in Fig. 6, the simulated spectra closely resemble the measured results, demonstrating the suitability of the chosen model as proposed by the XPS analysis. To further emphasize the goodness of the fit, the difference between the experimental and the simulated spectra is reported in Fig. 7. The observed scatter in the data with the angle of incidence reflects the inherent uniaxial anisotropy of the monolayer.[22] The results of the iterative fitting procedure indicate the presence of a SAM deposited from vapor phase with a thickness of 19.9 ± 0.2 Å and an oxide fraction of $8 \pm 2\%$. In addition, the best-fit model suggests that the monolayer is formed on a clean GaAs surface covered by a 106 ± 5 nm thick density-deficient layer, simulated by a mixture of $98.5 \pm 0.1\%$ GaAs and $1.5 \pm 0.1\%$ voids. The existence of a small amount of oxide in the multilayer model is in reasonable accord with the compositional data obtained from the XPS measurements. The presence of a porous interface layer correlates well with the expected interaction of atomic hydrogen with the GaAs substrate during the oxide removal process. Furthermore, it describes the modification of the optical properties at the surface evoked by the preferential reaction of hy-

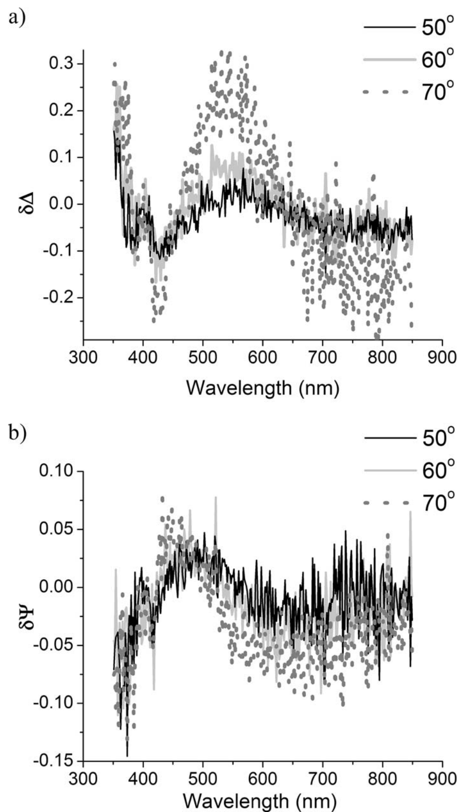

FIG. 7. Difference spectra (experimental–simulated) of ellipsometric parameters (a) Δ and (b) Ψ of a vapor-deposited ODT SAM on GaAs for various angles of incidence. For clarity, the spectra at angles of incidence of 55° and 65° have been excluded.

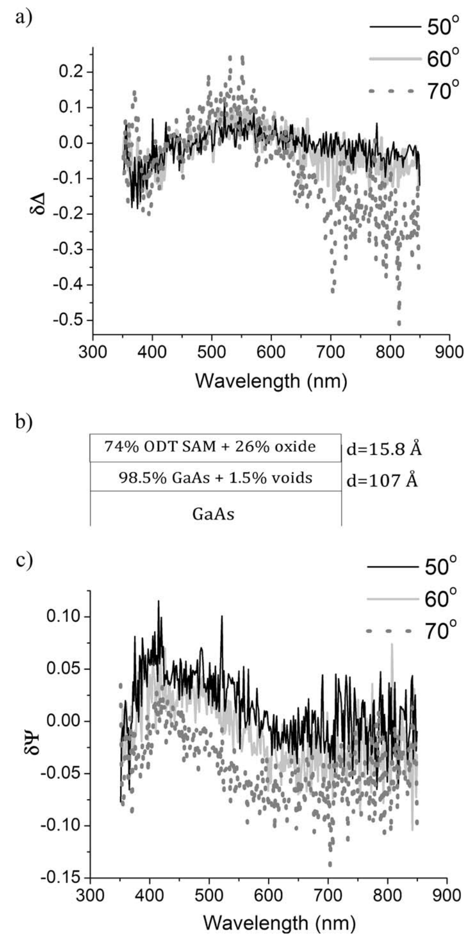

FIG. 8. Difference spectra (experimental–simulated) of ellipsometric parameters (a) Δ and (c) Ψ of an atomic-hydrogen-cleaned GaAs substrate for various angles of incidence. For clarity, the spectra at angles of incidence of 55° and 65° have been excluded. In (b) the best-fit BEMA model to the corresponding spectra is shown.

drogen with As and oxygen atoms, which leaves the surface nonstoichiometric and less dense.[49] The ready penetration of GaAs by atomic hydrogen accounts for the augmented thickness of the intermixed phase, as well as for surface roughening that may occur as a result of the treatment.[49] Likewise, the derived thickness of the vapor-deposited SAM is consistent with that reported in earlier studies.[13,48,50] The fact that the thickness of the film is smaller than the physical length of the octadecyl thiolate molecule (~24.5 Å) suggests the existence of a well-ordered monolayer on the GaAs surface consisting of densely packed alkyl chains tilted at $36 \pm 2°$ from the surface normal.

An analogous approach to the one described above was adapted to evaluate the spectra of the atomic-hydrogen-cleaned sample. Figure 8 depicts the difference between the ellipsometric data and the results of the regression analysis obtained with the model presented in the figure. The spectroscopic data suggest the formation of more disordered ODT assemblies separated by regions of GaAs oxide $(26 \pm 3\%)$ on the surface of the sample. The reduced thickness $(15.8 \pm 0.1$ Å) of the monolayer can likely be explained by a decrease in the tilt of the alkyl chains from the surface normal. Similar to the SAM deposited from vapor phase, the interface layer is modeled reasonably well by a mixture of GaAs and voids, which corresponds to the selective removal of As and oxygen atoms from the GaAs lattice during the exposure to atomic hydrogen.

To account for the apparent distinction in characteristics of the monolayers formed from solution as documented by means of PL spectroscopy and XPS, an alternative four-phase model was used to describe the properties of the solution-deposited SAM. Since the GaAs surface prior to SAM deposition from liquid phase is believed to be nearly stoichiometric, an interface layer was included in the ellipsometric model to allow for possible formation of a roughened overlayer, which has previously been shown to arise from the wet-etch oxide removal process.[51] As in the case of the vapor-deposited SAM, the effective refractive index of the monolayer was taken to be a weighted average of the refractive index of the GaAs oxide and the ODT, with the optical constants of the latter described by an equivalent Cauchy dispersion formula.

Figure 9 shows the difference spectra between the experimental and best-fit curves for Δ and Ψ of a film assembled from the thiol solution on GaAs. The good agreement between the measured and simulated data implies that the film

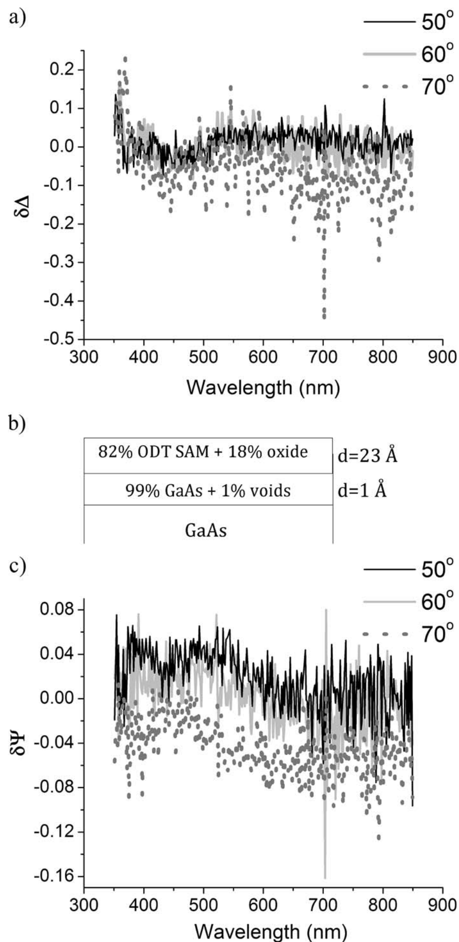

FIG. 9. Difference spectra (experimental–simulated) of ellipsometric parameters (a) Δ and (c) Ψ of a solution-deposited ODT SAM on GaAs for various angles of incidence. For clarity, the spectra at angles of incidence of 55° and 65° have been excluded. In (b) the best-fit BEMA model to the corresponding spectra is shown.

consists of less dense thiol domains with inclusions of a GaAs oxide. According to the ellipsometric model, the volume fraction of the GaAs oxide in the host medium was $18 \pm 1\%$, which is larger than that derived for the vapor-deposited SAM $(8 \pm 2\%)$. The best-fit model also indicates that the monolayer is formed on a roughened GaAs overlayer about 1 ± 0.5 Å thick, which is probably formed as a result of the HF etch used to strip the surface oxide prior to the assembly of the monolayer from solution. Furthermore, the increased thickness of the film of 23 ± 1 Å implies that the alkyl chains in the monolayer are tilted from the surface normal at a smaller angle of $20 \pm 2°$. Interestingly, this film thickness agrees well with that recently reported for an organized ODT monolayer on GaAs self-assembled from solution under similar preparation conditions.[15]

The results of the ellipsometric analysis, along with the experimental XPS data, suggest dissimilar structures for monolayers prepared from liquid and vapor phases. While conventional solution deposition yields a thicker monolayer with the axes of the thiolate molecules oriented nearly perpendicular to the sample surface, the overall coverage of the film is reduced. Conversely, the experimental data for the vapor-deposited monolayer are consistent with the presence of a thinner film composed of a densely packed assembly of molecules tilted more toward the sample surface. The superior characteristics of the vapor-deposited SAM inferred from the ellipsometric simulations correspond well to the larger enhancement in PL intensity observed for the monolayer when compared to that prepared from liquid phase. In the case of a solution-deposited monolayer, the greater oxide content of the SAM is likely related to the existence of weaker As–S bonds at the GaAs surface, which explains the decreased long-term stability of the film with exposure to an ambient environment, as was found through PL and CA analysis. On the other hand, the stronger Ga–S bonds formed between the vapor-deposited SAM and the GaAs substrate are responsible for the greater surface coverage of the film and directly translate to the improved passivation provided by these SAMs.

IV. CONCLUSION

The experimental data presented in this work suggest that the functionalization of GaAs with ODT SAMs inhibits the oxidization of the surface for an extended period of time and maintains a quality of the interface similar to that achieved via traditional oxide removal procedures. Although well-ordered films were formed from both liquid and vapor phases, PL, CA analysis, and ellipsometry measurements revealed that the overall quality of the resulting SAMs, as well as the long-term durability, depends on the preparation method. Specifically, time-dependent PL and CA analysis of the SAMs when exposed to the ambient environment indicate an increased stability for the vapor-deposited films when compared to the corresponding solution-deposited monolayers, which were shown to be more susceptible to atmospheric conditions over time. The film properties responsible for the difference in longevity of the resultant surface passivation were further explored by XPS. The attachment of the thiolate molecules to the GaAs surface was shown to proceed through the formation of chemical bonds as demonstrated by the appearance of the respective emissions in the Ga 3*d*, As 3*d*, and S 2*p* XPS spectra. Moreover, the anchoring of the thiols was observed to occur at both Ga and As adsorption sites and was found to be strongly dependent on the surface termination obtained by the particular oxide removal treatment used prior to the SAM deposition. While both preparation routes produced films with some residual oxide contamination, vapor-deposited SAMs were found to have greater surface coverage and enhanced passivation properties, as confirmed by ellipsometry and improved PL peak intensity. From the XPS results, the superior characteristics of films prepared from vapor phase were linked to the dominant formation of robust Ga–S bonds at the GaAs-SAM interface. Consequently, the preparation of high-quality organic SAMs from vapor phase is a promising strategy for the reliable passivation of semiconductor surfaces and a prospective means of enhancing the performance and stability of III-V-based devices.

ACKNOWLEDGMENTS

Funding for this research was provided by the Natural Sciences and Engineering Research Council of Canada. Spectroscopic ellipsometry measurements reported in this work were performed with the assistance of Jacek Wojcik. The authors also wish to thank Brad Robinson for his assistance with the vapor deposition and PL experiments, as well as for the informative discussions.

[1]G. Bruno, P. Capezzuto, and M. Losurdo, Vacuum **57**, 189 (2000).
[2]M. Kang and H. Park, Jpn. J. Appl. Phys. **40**, 4454 (2001).
[3]S. Anantathanasarn and H. Hasegawa, Appl. Surf. Sci. **190**, 343 (2002).
[4]S. Arabasz, E. Bergignat, G. Hollinger, and J. Szuber, Vacuum **80**, 888 (2006).
[5]C. Ashby, K. Zavadil, A. Baca, P. Chang, B. Hammons, and M. Hafich, Appl. Phys. Lett. **76**, 327 (2000).
[6]O. Dassa, V. Sidorov, Y. Paz, and D. Ritter, J. Electrochem. Soc. **153**, G91 (2006).
[7]K. Butcher, R. Egan, T. Tansley, and D. Alexiev, J. Vac. Sci. Technol. B **14**, 152 (1996).
[8]M. Kang, J. Kim, and H. Park, Jpn. J. Appl. Phys. **39**, 7003 (2000).
[9]R. Gottscho, B. Preppernau, S. Pearton, A. Emerson, and K. Giapis, J. Appl. Phys. **68**, 440 (1990).
[10]S. Lunt, P. Santangelo, and N. Lewis, J. Vac. Sci. Technol. B **9**, 2333 (1991).
[11]K. Adlkofer, E. Duijs, F. Findeis, M. Bichler, A. Zrenner, E. Sackmann, G. Abstreiter, and M. Tanaka, Phys. Chem. Chem. Phys. **4**, 785 (2002).
[12]X. Ding and J. Dubowski, Proc. SPIE **5713**, 545 (2005).
[13]K. Adlkofer and M. Tanaka, Langmuir **17**, 4267 (2001).
[14]J. Dorsten, J. Maslar, and P. Bohn, Appl. Phys. Lett. **66**, 1755 (1995).
[15]C. McGuiness, A. Shaporenko, C. Mars, S. Uppili, M. Zharnikov, and D. Allara, J. Am. Chem. Soc. **128**, 5231 (2006).
[16]H. Ohno, M. Motomatsu, W. Mizutani, and H. Tokumoto, Jpn. J. Appl. Phys., Part 1 **34**, 1381 (1995).
[17]K. Remashan and K. Bhat, Thin Solid Films **342**, 20 (1999).
[18]S. Ye, G. Li, H. Noda, K. Uosaki, and M. Osawa, Surf. Sci. **529**, 163 (2003).
[19]D. Wieliczka, X. Ding, and J. Dubowski, J. Vac. Sci. Technol. A **24**, 1756 (2006).
[20]Wafer Technology Ltd., 34 Maryland Road, Tongwell, Milton Keynes, Bucks MK15 8HJ, United Kingdom (http://www.wafertech.co.uk/).
[21]Sigma-Aldrich, 3050 Spruce Street, St. Louis, MO 63103 (http://www.sigmaaldrich.com/).
[22]H. Budz and R. LaPierre, J. Vac. Sci. Technol. A **26**, 1425 (2008).
[23]N. Razek, K. Otte, T. Chasse, D. Hirsch, A. Schindler, F. Frost, and B. Rauschenbach, J. Vac. Sci. Technol. A **20**, 1492 (2002).
[24]J. A. Woollam Co., Inc., 645 M Street, Suite 102, Lincoln, NE 68508-2243 (http://www.jawoollam.com/).
[25]Sciencetech Inc., 60 Meg Drive, London, ON N6E 3T6, Canada (http://www.sciencetech-inc.com/).
[26]T. Hou, C. Greenlief, S. Keller, L. Nelen, and J. Kauffman, Chem. Mater. **9**, 3181 (1997).
[27]O. Nakagawa, S. Ashok, C. Sheen, J. Märtensson, and D. Allara, Jpn. J. Appl. Phys. **30**, 3759 (1991).
[28]C. Kirchner, M. George, B. Stein, W. Parak, H. Gaub, and M. Seitz, Adv. Funct. Mater. **12**, 266 (2002).
[29]C. Wagner, A. Naumkin, A. Kraut-Vass, J. Allison, C. Powell, and J. Rumble, NIST X-ray Photoelectron Spectroscopy Database, The Measurement Services Division of the National Institute of Standards and Technology (online), August 27, 2007 (http://srdata.nist.gov/xps) (accessed August 25, 2008).
[30]S. Ghosh, M. Biesinger, R. LaPierre, and P. Kruse, J. Appl. Phys. **101**, 114322 (2007).
[31]C. McGuiness, A. Shaporenko, M. Zharnikov, A. Walker, and D. Allara, J. Phys. Chem. C **111**, 4226 (2007).
[32]Y. Gu and D. Waldeck, J. Phys. Chem. B **102**, 9015 (1998).
[33]C. Hamilton, S. Hicks, B. Vogele, J. Marsh, and J. Aitchison, Electron. Lett. **31**, 1393 (1995).
[34]M. Yamada, Y. Ide, and K. Tone, Jpn. J. Appl. Phys., Part 2 **31**, L1157 (1992).
[35]E. Yoon, R. Gottscho, V. Donnelly, and H. Luftman, Appl. Phys. Lett. **60**, 2681 (1992).
[36]M. Losurdo, P. Capezzuto, and G. Bruno, Thin Solid Films **313–314**, 501 (1998).
[37]Veeco Application Note No. 3/98 (online), September 1998 (http://www.veeco.com/pdfs/appnotes/98sept_ahs_78.pdf) (accessed September 13, 2008).
[38]A. Chanda, S. Verma, and C. Jacob, Bull. Mater. Sci. **30**, 561 (2007).
[39]D. Gräf, M. Grundner, D. Lüdecke, and R. Schulz, J. Vac. Sci. Technol. A **8**, 1955 (1990).
[40]J. Shin, K. Geib, and C. Wilmsen, J. Vac. Sci. Technol. B **9**, 2337 (1991).
[41]O. Voznyy and J. Dubowski, J. Phys. Chem. C **112**, 3726 (2008).
[42]H. Sik, Y. Feurprier, C. Cardinaud, G. Turban, and A. Scavenne, J. Electrochem. Soc. **144**, 2106 (1997).
[43]I. Gouzman, M. Dubey, M. Carolus, J. Schwartz, and S. Bernasek, Surf. Sci. **600**, 773 (2006).
[44]M. Rei Vilar, J. Beghdadi, F. Debontridder, R. Artzi, R. Naaman, A. Ferraria, and A. Botelho do Rego, Surf. Interface Anal. **37**, 673 (2005).
[45]Y. Jun, X. Zhu, and J. Hsu, Langmuir **22**, 3627 (2006).
[46]M. Kuball, M. Kelly, P. Santos, and M. Cardona, Phys. Rev. B **50**, 8609 (1994).
[47]G. Bruno, P. Capezzuto, and M. Losurdo, Phys. Rev. B **54**, 17175 (1996).
[48]J. Shi, B. Hong, A. Parikh, R. Collins, and D. Allara, Chem. Phys. Lett. **246**, 90 (1995).
[49]P. Snyder, N. Ianno, B. Wigert, S. Pittal, B. Johs, and J. Woollam, J. Vac. Sci. Technol. B **13**, 2255 (1995).
[50]S. Lodha and D. Janes, Proceedings of the Fourth IEEE Conference on Nanotechnology, 2004 (unpublished), p. 278.
[51]S. Adachi and D. Kikuchi, J. Electrochem. Soc. **147**, 4618 (2000).